Incorporating seismic interferometry and full waveform inversion

Jinji Li and Kristopher A. Innanen

ABSTRACT

Seismic interferometry, through the cross-correlation of data recorded by receiver pairs, can extract Green's function, enabling the potential redatuming of signals using passive datasets. This capability holds promise for integration with full waveform inversion (FWI) to continuously update subsurface property estimates in real time. This report presents a preliminary investigation into the feasibility of combining seismic interferometry and FWI by introducing a novel objective function aimed at mitigating interference patterns in seismic waveforms. A straightforward numerical example demonstrates that, under conventional surface acquisition constraints, seismic interferometry can enhance the estimation of P-wave velocity. However, further comprehensive research is needed to assess the algorithm's performance across diverse scenarios, including elastic applications.

INTRODUCTION

Seismic monitoring with full waveform inversion (FWI) represents a cutting-edge approach to seismic exploration and reservoir management (e.g., (Boullenger et al., 2014; Nishida et al., 2020; Henley and Lawton, 2021)). FWI leverages the full complexity of seismic data, capturing a wealth of information about subsurface properties such as rock composition, fluid content, and structural details with unparalleled precision. Nonetheless, realizing the full potential of FWI is not a straightforward task. It demands a continuous stream of high-quality seismic data and the regular refinement of subsurface models. This necessity arises from the inherent complexity of Earth's subsurface, which is dynamic and subject to various influences, such as changing reservoir conditions or external seismic events. Therefore, the seamless integration of ongoing data acquisition and model updates becomes paramount in making FWI a practical tool in the field.

One of the key elements that make this integration feasible and efficient is seismic interferometry. Seismic interferometry is a technique that can be applied to estimate the properties of the earth by analyzing the interference patterns of seismic waves (Schuster, 2009). By cross-correlating and summing pairs of seismic traces, it is possible to create a synthetic response between any two receivers, effectively treating one of them as a virtual source (Wapenaar et al., 2010). Hence, it doesn't require costly and often environmentally disruptive active seismic sources, as it can make use of ambient seismic noise, such as ocean waves, traffic, or even the Earth's natural vibrations. This technique has been utilized in various fields, including ultrasonics (Weaver and Lobkis, 2001; van Wijk, 2006), global seismology (Sabra et al., 2005; Shapiro et al., 2005), and ocean acoustics (Roux et al., 2004; Sabra et al., 2005). Reviews of interferometry across multiple disciplines can be found in (Curtis et al., 2006) and (Larose et al., 2004). As understanding of the method advances, new applications become possible, such as its potential use in reservoir engineering, as demonstrated by Snieder and safak (2006), who showed that interferometry principles also apply to the diffusion equation. The redatuming capability also opens up the possibility

of using a combination of seismic interferometry and passive FWI (e.g. (Draganov et al., 2004)) for long-term monitoring of changes in a specific area.

The integration of FWI and seismic interferometry offers a possible solution to monitor subsurface reservoirs in real time, tracking changes in fluid content, pressure, and other critical parameters with a reasonable degree of accuracy. Moreover, it enhances our capability to assess seismic hazard potential by continuously updating seismic velocity models, helping us understand and mitigate earthquake risks more effectively. In this report, we conduct a preliminary study on the integration of seismic interferometry and Full Waveform Inversion (SI-FWI) for estimating acoustic properties. We illustrate the application of seismic interferometry in acoustic media and introduce a new objective function to minimize interference patterns between synthetic and observed data. A simple numerical example demonstrates the feasibility of SI-FWI, with discussions on potential future work.

THEORY

From reciprocity theorem to seismic interferometry

Numerous papers have demonstrated that by cross-correlating two recordings of a dispersed wavefield at two different receiver locations, one can obtain the Green's function that would be detected at one of these receiver locations in the presence of an impulsive source at the other. The diffusive nature of a wavefield can arise from a range of phenomena, such as the stochastic distribution of uncorrelated noise sources (Weaver and Lobkis, 2001; Wapenaar, 2006; Roux et al., 2004; Shapiro et al., 2005), reverberations within an enclosure that features an irregular boundary surface (Lobkis and Weaver, 2001), multiple scattering between heterogeneous elements in a disordered medium (Campillo and Paul, 2003), or a combination of these factors.

This section is an overview of representations of Green's functions regarding cross-correlations of full wavefields. In order to distinguish seismic interferometry from other methods, it is crucial to begin with the basics, namely the reciprocity theorems. By grasping these principles, one can gain an understanding of seismic interferometry.

The reciprocity theorem can be derived in both elastic and acoustic media (Wapenaar, 2006). We start with deriving the acoustic reciprocity theorem and then talk about the essential approximations that lead to the applicable seismic interferometry.

Consider a lossless inhomogeneous anisotropic medium, a wavefield u characterized in this medium obeys the equation of motion:

$$j\omega\rho v_i + \partial_i u = f_i, \tag{1}$$

and the stress-strain relation:

$$j\omega\kappa\rho u + \partial_i v_i = q, \tag{2}$$

where ω is the angular frequency, ρ is the density, v_i is particle velocity, f_i is the external source, κ is compressibility, q is the volume injection rate, and j is the complex unit (Wapenaar, 2006).

Consider two independent states A and B where the physical parameters are identical, the interaction quantity can be given as:

$$\partial_i \left(u_A v_{i,B} - v_{i,A} u_B \right). \tag{3}$$

Substituting equation 1 and 2 into equation 3, and integrate the result over an arbitrary D enclosed by ∂D gives:

$$\int_D \left(f_{i,A} v_{i,B} + u_A q_B - q_A u_B - v_{i,A} f_{i,B} \right) d^3\mathbf{x}. \tag{4}$$

Subsequently, apply the theorem of Gauss:

$$\oint_{\partial D} \left(u_A v_{i,B} - v_{i,A} u_B \right) n_i d^2\mathbf{x}. \tag{5}$$

This is the reciprocity theorem of the convolution type (Aki and Richards, 2002).

Assuming the seismic medium is lossless such that the time reversal can be applied to either of the states. The time-reversed volume injection rate should be negative-conjugated, thus, the solution of particle velocity in equation 2 is $-v_i^*$ where the asteroid denotes complex conjugate. Substituting the time-reversed state A into equation 3 and following the same procedure in deriving equation 4 and equation 5 gives the correlational reciprocity theorem (Wapenaar, 2006):

$$\int_D \left(f_{i,A} v_{i,B} + u_A q_B + q_A u_B + v_{i,A} f_{i,B} \right) d^3\mathbf{x} = \oint_{\partial D} \left(u_A^* v_{i,B} - v_{i,A}^* u_B \right) n_i d^2\mathbf{x}. \tag{6}$$

Under an open configuration (Wapenaar, 2006) where the boundary ∂D is a subdomain but does not necessarily coincide with a physical boundary of D, the representations of Green's functions using interferometry can be derived using the reciprocity theorems. Assume two impulsive point sources of volume injection rate in both states in the frequency domain:

$$q_A \left(\mathbf{x}, \omega \right) = \delta \left(\mathbf{x} - \mathbf{x}_A \right), \tag{7}$$

$$q_B \left(\mathbf{x}, \omega \right) = \delta \left(\mathbf{x} - \mathbf{x}_B \right), \tag{8}$$

The wavefield excited in states A and B can be represented in terms of Green's functions: The wavefield excited in states A and B can be represented in terms of Green's functions:

$$u_A \left(\mathbf{x}, \omega \right) = G \left(\mathbf{x}_A, \mathbf{x}, \omega \right), \tag{9}$$

$$u_B \left(\mathbf{x}, \omega \right) = G \left(\mathbf{x}_B, \mathbf{x}, \omega \right), \tag{10}$$

with the assumption that the external force is zero in both states, the particle velocities can be expressed as:

$$v_{i,A} \left(\mathbf{x}, \omega \right) = -\frac{1}{j\omega\rho} \partial_i G \left(\mathbf{x}_A, \mathbf{x}, \omega \right), \tag{11}$$

$$v_{i,B}\left(\mathbf{x},\omega\right)=-\frac{1}{j\omega\rho}\partial_i G\left(\mathbf{x}_B,\mathbf{x},\omega\right). \tag{12}$$

The source-receiver reciprocity can be derived by substituting equation 9 - equation 12 to the convolutional reciprocity theorem:

$$\begin{aligned}-G\left(\mathbf{x}_B,\mathbf{x}_A,\omega\right)+G\left(\mathbf{x}_A,\mathbf{x}_B,\omega\right)=\oint_{\partial D}-\frac{1}{j\omega\rho}[&G\left(\mathbf{x},\mathbf{x}_A,\omega\right)\partial_i G\left(\mathbf{x},\mathbf{x}_B,\omega\right)\\&-\partial_i G\left(\mathbf{x},\mathbf{x}_A,\omega\right)G\left(\mathbf{x},\mathbf{x}_B,\omega\right)]n_i d^2\mathbf{x}.\end{aligned} \tag{13}$$

The right-hand side of equation 14 can be omitted since it is independent of the selection of ∂D. It vanishes when ∂D is the margin of a spherical district with near-infinite radius, thus leading to:

$$G\left(\mathbf{x}_A,\mathbf{x}_B,\omega\right)=G\left(\mathbf{x}_B,\mathbf{x}_A,\omega\right) \tag{14}$$

Substituting equation 9 - equation 13 into the correlation-type reciprocal theorem gives:

$$\begin{aligned}G^*\left(\mathbf{x}_B,\mathbf{x}_A,\omega\right)+G\left(\mathbf{x}_A,\mathbf{x}_B,\omega\right)=\oint_{\partial D}-\frac{1}{j\omega\rho}[&G^*\left(\mathbf{x},\mathbf{x}_A,\omega\right)\partial_i G\left(\mathbf{x},\mathbf{x}_B,\omega\right)\\&-\partial_i G^*\left(\mathbf{x},\mathbf{x}_A,\omega\right)G\left(\mathbf{x},\mathbf{x}_B,\omega\right)]n_i d^2\mathbf{x}.\end{aligned} \tag{15}$$

The existence of the anti-causal Green's functions in equation 16 means the right-hand side cannot vanish (Wapenaar, 2006). Applying the source-receiver reciprocity relation yields:

$$\begin{aligned}G^*\left(\mathbf{x}_A,\mathbf{x}_B,\omega\right)+G\left(\mathbf{x}_A,\mathbf{x}_B,\omega\right)=\oint_{\partial D}-\frac{1}{j\omega\rho}[&G^*\left(\mathbf{x}_A,\mathbf{x},\omega\right)\partial_i G\left(\mathbf{x}_B,\mathbf{x},\omega\right)\\&-\partial_i G^*\left(\mathbf{x}_A,\mathbf{x},\omega\right)G\left(\mathbf{x}_B,\mathbf{x},\omega\right)]n_i d^2\mathbf{x}.\end{aligned} \tag{16}$$

Equation 16 is the basis of the acoustic seismic interferometry, as the right-hand side can be interpreted as the integral along the source coordinate $\mathbf{x}$ of the cross-correlations of the observed wavefields at $\mathbf{x}_A$ and $\mathbf{x}_B$ excited by impulsive sources located at ∂D. The reconstructed Green's function contains not only the direct wave between $\mathbf{x}_A$ and $\mathbf{x}_B$, but also all scattering contributions from homogeneities inside as well as outside ∂D. However, the right-hand side in equation 16 is too complex to be implemented, as it contains the spatial derivative of Green's functions. Additionally, the term $G^*\partial_i G n_i$ represents the cross-correlation between Green's functions excited by monopole and dipole sources, which also increases the complexity.

Consider one source point on ∂_D illustrated by Figure 1, where the outward-pointing vector $\mathbf{n}$ is perpendicular to the surface. The Green's functions from this source to two different locations A and B can be represented by $G\left(\mathbf{x}_A,\mathbf{x},\omega\right)$ and $G\left(\mathbf{x}_B,\mathbf{x},\omega\right)$, respectively. The response between A and B is $G\left(\mathbf{x}_A,\mathbf{x}_B,\omega\right)$. Figure 2 exhibits that, the response from a source at ∂_D to an arbitrary location inside D can be separated into inward and outward components, where the outward component is scattered by inhomogeneities outside D (Wapenaar, 2006). Accordingly, the Green's functions at A and B can be rewritten as:

$$G\left(\mathbf{x}_A,\mathbf{x},\omega\right)=G^{in}\left(\mathbf{x}_A,\mathbf{x},\omega\right)+G^{out}\left(\mathbf{x}_A,\mathbf{x},\omega\right), \tag{17}$$

$$G\left(\mathbf{x}_B,\mathbf{x},\omega\right)=G^{in}\left(\mathbf{x}_B,\mathbf{x},\omega\right)+G^{out}\left(\mathbf{x}_B,\mathbf{x},\omega\right). \tag{18}$$

Under the assumption that the spherical D with a large radius is an open configuration, and that ∂_D is smooth, the normal derivatives of Green's functions from $\mathbf{x}$ to $\mathbf{x}'$ can be approximated with the far-field assumption (**?**Wapenaar, 2006; Snieder, 2006; **?**):

$$\partial_i G\left(\mathbf{x}', \mathbf{x}, \omega\right) = \pm j k_i, \tag{19}$$

where the normal wavenumber $k_i = \frac{\omega}{c}\left|\cos\theta\right|$, with c being the wave propagation speed, and θ being the local angle between the pertinent ray and the normal on ∂_D. Previous studies have shown that the main contributions to the integral in equation 16 come from stationary points on ∂_D, where the absolute values of $\cos\theta$ are equal (Snieder and safak, 2006). Hence, the products such as $G^{in^*}\partial_i G_{out} n_i$ and $-G^{out}\partial_i G_{in^*} n_i$ can cancel each other. Substituting equation 17, equation 18, and equation 19 into equation 16, and re-organizing the result gives:

$$\begin{aligned} G^*\left(\mathbf{x}_A, \mathbf{x}_B, \omega\right) + G\left(\mathbf{x}_A, \mathbf{x}_B, \omega\right) = & \oint_{\partial D} \frac{2}{j\omega\rho} \partial_i G^*\left(\mathbf{x}_A, \mathbf{x}, \omega\right) G\left(\mathbf{x}_B, \mathbf{x}, \omega\right) n_i d^2\mathbf{x} \\ & - \oint_{\partial D} \frac{2}{j\omega\rho} [\partial_i G^{in^*}\left(\mathbf{x}_A, \mathbf{x}, \omega\right) G^{out}\left(\mathbf{x}_B, \mathbf{x}, \omega\right) \\ & - \partial_i G^{out^*}\left(\mathbf{x}_A, \mathbf{x}, \omega\right) G^{in}\left(\mathbf{x}_B, \mathbf{x}, \omega\right)] n_i d^2\mathbf{x}. \end{aligned} \tag{20}$$

The second integral contains cross-correlations of inward and outward propagating wavefields. However, when ∂_D is irregular, this integral is not sufficiently influential to the retrieved Green's functions, thus, can be omitted. Draganov et al. (2006) have exhibited that the reconstructed Green's functions include all the scattering effects from both sides of ∂_D.

The dipole response, as shown by the normal derivative term, can be approximated by the monopole response:

$$\partial_i G\left(\mathbf{x}', \mathbf{x}, \omega\right) n_i \approx -j\frac{\omega}{c} G\left(\mathbf{x}', \mathbf{x}, \omega\right), \tag{21}$$

thus leads to:

$$G^*\left(\mathbf{x}_A, \mathbf{x}_B, \omega\right) + G\left(\mathbf{x}_A, \mathbf{x}_B, \omega\right) \approx \oint_{\partial D} \frac{2}{\rho c} G^*\left(\mathbf{x}_A, \mathbf{x}, \omega\right) G\left(\mathbf{x}_B, \mathbf{x}, \omega\right) d^2\mathbf{x}. \tag{22}$$

This approximation makes seismic interferometry more applicable. It infers that Green's function between two arbitrary locations inside an area D can be reconstructed by integral on the cross-correlated wavefields at these locations. However, spurious events might occur due to the incomplete cancellation from different stationary points around the boundary ∂_D, which may pose a practical limitation. Longer recording time and more comprehensive acquisition systems can help compensate for this problem (**?**). Although spurious events cannot always be eliminated, equation 22 is considered acceptable and practical because the numerical errors do not significantly influence the kinematics, and the amplitude correction term $\frac{2}{\rho c}$ can be omitted for the same reason.

Derivation of SI-FWI

In this section, we show a preliminary study of integrating seismic interferometry and FWI (SI-FWI) in estimating acoustic properties. A new objective function is designed to

minimize the interference patterns between the synthetic and observed data. The feasibility is shown by a simple numerical example, although further studies, such as incorporating source inversion, elastic SI-FWI, and more comprehensive experiments, are required. In frequency domain, the wavefield with an excitation at $\mathbf{s}$ and recorded at $\mathbf{r}_A$ can be regarded as the pressure response in acoustic media from $\mathbf{s}$ to $\mathbf{r}_A$ multiplied with a source function $W(\mathbf{s},\omega)$ (Wapenaar, 2006):

$$u(\mathbf{r}_A,\mathbf{s},\omega) = W(\mathbf{s},\omega)\, G(\mathbf{r}_A,\mathbf{s},\omega). \tag{23}$$

The crosscorrelation of wavefields measured at $\mathbf{r}_A$ and generated at another receiver $\mathbf{r}_B$ is given by:

$$C_{AB} = |W(\mathbf{s})|^2\, G(\mathbf{r}_A,\mathbf{s},\omega)\, G^*(\mathbf{r}_B,\mathbf{s},\omega), \tag{24}$$

where the asterisk denotes complex conjugate. A close integration of equation 19 over a surface V that contains all the source $\mathbf{s}$ gives:

$$\oint_{\partial V} C_{AB} d\mathbf{s} = \left\langle |W(\mathbf{s})|^2 \right\rangle \left[G(\mathbf{r}_A,\mathbf{r}_B,\omega) + G^*(\mathbf{r}_A,\mathbf{r}_B,\omega) \right], \tag{25}$$

where $\left\langle |W(\mathbf{s})|^2 \right\rangle$ is the source average of the power spectra (Snieder, 2006). $G(\mathbf{r}_A,\mathbf{r}_B,\omega)$, and $G^*(\mathbf{r}_A,\mathbf{r}_B,\omega)$ are the causal and anti-causal response measured at $\mathbf{r}_A$ with $\mathbf{r}_B$ being a virtual source. Hence, it is reasonable to form an objective function that aims to minimize the interferometric data residual. Recall the synthetic data excited at arbitrary source $\mathbf{s}$ can be acquired by applying a sampling matrix R to the wavefield $u(\mathbf{s},\omega)$. Omitting the frequency dependence, the components in the interferometry matrix can be derived by a matrix multiplication between d and $d^\dagger$:

$$C_{i,j} = \sum_k^{Ns} \left(d_{i,k} d^*_{k,j} \right) = \sum_k^{Ns} \left(R_{i,l} u_{l,k} u^*_{k,l} R_{l,j} \right). \tag{26}$$

This process implicitly accounts for the source integration in equation 25. Hence:

$$\oint_{\partial V} C_{AB} d\mathbf{s} = d(\mathbf{r}_A,\omega)\, d^\dagger(\mathbf{r}_B,\omega) = Ru(\mathbf{s},\omega)\, u^\dagger(\mathbf{s},\omega)\, R^T. \tag{27}$$

Such formulation allows us to build a new optimization problem aiming at minimizing the discrepancy between interferometry patterns. For simplicity, we consider the below objective function in one frequency:

$$\min_{\mathbf{x}} \Phi(\mathbf{x}) = \min_{\mathbf{x}} \frac{1}{2} \| Ruu^\dagger R^T - C_0 \|_2^2, \text{ s.t. } S(\mathbf{x})u = f, \tag{28}$$

where C_0 is calculated by $d_{obs} d^\dagger_{obs}$. It is important to note that this problem is subject to the wave equation, which might utilize the original source vector to perform passive FWI through arbitrary excitations. The adjoint wavefield $\overline{\kappa}$ and gradient $\mathbf{g}$ with respect to model parameter can be represented:

$$\overline{\kappa} = 2R^T \left[R\overline{u} \left(R\overline{u} \right)^\dagger - C_0 \right] R\overline{u}, \tag{29}$$

$$\mathbf{g} = \left\langle \frac{\partial S}{\partial \mathbf{m}} \overline{u}, \overline{\kappa} \right\rangle. \tag{30}$$

Numerical examples

We first demonstrate redatuming using seismic interferometry on a 2-layered model depicted in Figure 1. The acquisition system comprises of one source, represented by the blue asteroid, and 48 receivers, denoted by red triangles. In essence, the application of interferometry eliminates the ray path from the source to every receiver (as indicated by the black arrow), resulting in a new set of ray paths between any two receivers in the array as shown by the light blue arrow.

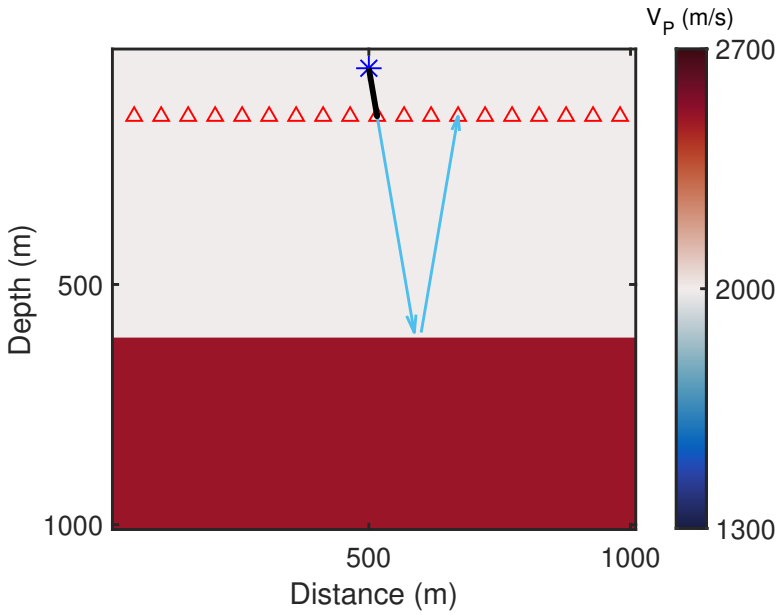

FIG. 1. 2-layered velocity model and schematic acquisition.

Figure 2 displays two shot gathers: one from the original source, and the other from the middle receiver acting as the virtual source. After applying interferometry, the receiver array is also considered a shot array, so the direct arrivals in the redatumed shot gather come from the virtual sources. Accordingly, the reflection time is also shifted, as shown in Figure 2 (b).

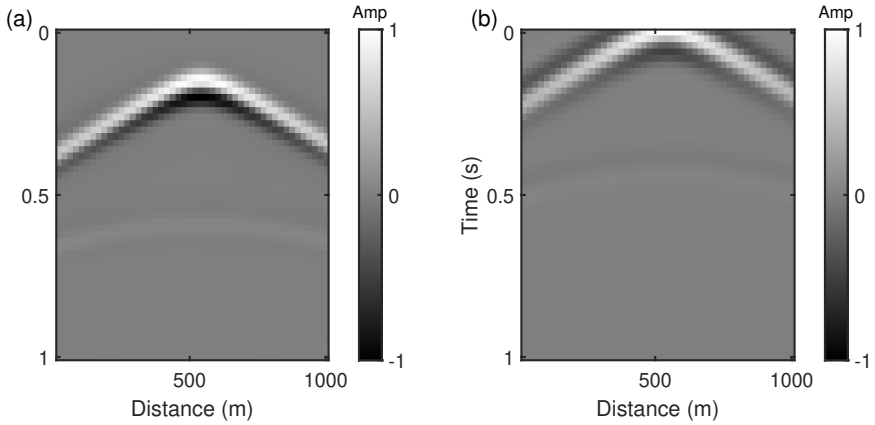

FIG. 2. Shot gathers. (a) Original shot gather. (b) Redatumed shot gather with virtual source in the 23rd receiver. The amplitude is normalized.

Next, we show the SI-FWI on an acoustic model with a circle abnormaly in the center part. The close surface integral in equation 25 is for correcting for medium perturbations located on the stationary paths of unperturbed waves that propagate from sources $\mathbf{s}$ to receivers $\mathbf{r}$ (Vasconcelos and Snieder, 2008). However, a partial source integration is more applicable in practice, although the truncation of the surface integral may introduce spurious events in the interferometric gathers (Snieder et al., 2006a,b), which may have negative influence on the FWI. We consider some acquisition systems with various source number, as illustrated by the first column of Figure 3. By including more sources, a more thorough partial source integration can be implemented, resulting in increased accuracy of the SI-FWI. It is reasonable to infer that interferometric shot gathers have the same number of sources as recorders, thereby furnishing the inversion with a more feasible amount of information. Additionally, in this numerical experiment, both the original and the interferometric acquisition systems are dominated by reflections, leading to a more accurate estimation of the upper section of the anomaly.

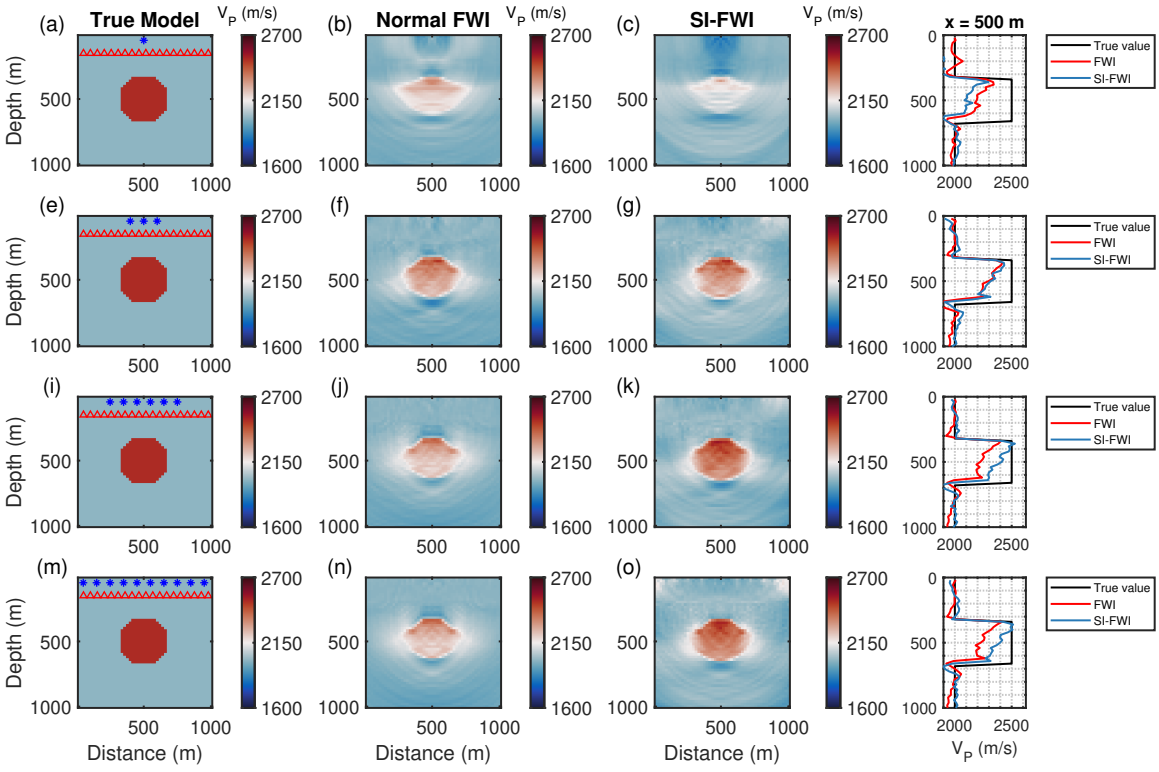

FIG. 3. SI-FWI tests. The first column ((a), (e), (i), (m)) shows the true model and acquisitions with various source number. The second column ((b), (f), (j), (n)) shows the results of conventional FWI. The third column ((c), (g), (k), (o)) shows SI-FWI results. The last column shows the vertical profile at x = 500 m, with the black lines from the true model, the red lines from the conventional FWI, and the light blue lines from the SI-FWI.

CONCLUSIONS

This preliminary assessment suggests that the SI-FWI approach holds promise for further development. However, several critical issues demand careful consideration and resolution. Firstly, it is imperative to derive second-order derivative terms to bolster the robustness of the inversion process, enhancing its reliability when applied to intricate models

or multi-parameter inversion scenarios. Secondly, when integrating elastic interferometry with FWI, the conversion of different wave components must be addressed to ensure compatibility. Thirdly, incorporating source estimation is essential to tackle source-related challenges in passive FWI. Lastly, it is imperative to identify and elucidate the limitations inherent in this approach.

Future research endeavors will be dedicated to exploring the potential of the SI-FWI approach for various applications requiring long-term monitoring. One potential extension of this FWI scheme involves the integration of deconvolutional interferometry, which can mitigate source uncertainty by eliminating the influence of source wavelet spectra. While this algorithm is more intricate than cross-correlational methods, it proves beneficial in mitigating source uncertainty in time-lapse monitoring by internally eliminating dependence on wavelet spectra. Additionally, exploring the integration of source inversion into SI-FWI to expand its capabilities will be a worthwhile pursuit.

ACKNOWLEDGEMENTS

We thank the sponsors of CREWES for continued support. This work was funded by CREWES industrial sponsors and NSERC (Natural Science and Engineering Research Council of Canada) through the grant CRDPJ 543578-19.

One of the authors of this report was supported by the CSEG Foundation.

REFERENCES

Aki, K., and Richards, P., 2002, Quantitative Seismology, Geology Seismology: University Science Books.

Boullenger, B., Verdel, A., Paap, B., Thorbecke, J., and Draganov, D., 2014, Studying co2 storage with ambient-noise seismic interferometry: A combined numerical feasibility study and field-data example for ketzin, germany: Geophysics, **80**, Q1–Q13.

Campillo, M., and Paul, A., 2003, Long-range correlations in the diffuse seismic coda: Science (New York, N.Y.), **299**, 547–9.

Curtis, A., Gerstoft, P., Sato, H., Snieder, R., and Wapenaar, K., 2006, Seismic interferometry—turning noise into signal: The Leading Edge, **25**, No. 9, 1082–1092.

Draganov, D., Wapenaar, K., and Thorbecke, J., 2004, Passive seismic imaging in the presence of white noise sources: The Leading Edge, **23**, No. 9, 889–892.

Draganov, D., Wapenaar, K., and Thorbecke, J., 2006, Seismic interferometry: Reconstructing the earth's reflection response: Geophysics, **71**, No. 4, SI61–SI70.

Henley, D. C., and Lawton, D. C., 2021, Time-lapse detection using raypath interferometry: GEOPHYSICS, **86**, No. 2, Q27–Q36.

Larose, E., Arnaud, D., Campillo, M., and Fink, M., 2004, Imaging from one-bit correlation of wide-band diffuse wavefield: Journal of Applied Physics - J APPL PHYS, **95**.

Lobkis, O. I., and Weaver, R. L., 2001, On the emergence of the Green's function in the correlations of a diffuse field: The Journal of the Acoustical Society of America, **110**, No. 6, 3011–3017, `https://pubs.aip.org/asa/jasa/article-pdf/110/6/3011/8089727/3011_1_online.pdf`.
URL `https://doi.org/10.1121/1.1417528`

Nishida, K., Mizutani, Y., Ichihara, M., and Aoki, Y., 2020, Time-lapse monitoring of seismic velocity associated with 2011 shinmoe-dake eruption using seismic interferometry: An extended kalman filter approach: Journal of Geophysical Research: Solid Earth, **125**, No. 9, e2020JB020,180.

Roux, P., Kuperman, W., and Group, N., 2004, Extracting coherent wave fronts from acoustic ambient noise in the ocean: Journal of the Acoustical Society of America, **116**, 1995–2003.

Sabra, K. G., Gerstoft, P., Roux, P., Kuperman, W. A., and Fehler, M. C., 2005, Surface wave tomography from microseisms in southern california: Geophysical Research Letters, **32**, No. 14.

Schuster, G. T., 2009, Seismic Interferometry: Cambridge University Press.

Shapiro, N. M., Campillo, M., Stehly, L., and Ritzwoller, M. H., 2005, High-resolution surface-wave tomography from ambient seismic noise: Science, **307**, No. 5715, 1615–1618.

Snieder, R., 2006, Retrieving the green's function of the diffusion equation from the response to a random forcing: Physical review. E, Statistical, nonlinear, and soft matter physics, **74**, 046,620.

Snieder, R., and safak, E., 2006, Extracting the Building Response Using Seismic Interferometry: Theory and Application to the Millikan Library in Pasadena, California: Bulletin of the Seismological Society of America, **96**, No. 2, 586–598.

Snieder, R., Sheiman, J., and Calvert, R., 2006a, Equivalence of the virtual-source method and wave-field deconvolution in seismic interferometry: Phys. Rev. E, **73**, 066,620.

Snieder, R., Wapenaar, K., and Larner, K., 2006b, Spurious multiples in seismic interferometry of primaries: GEOPHYSICS, **71**, No. 4, SI111–SI124.

van Wijk, K., 2006, On estimating the impulse response between receivers in a controlled ultrasonic experiment: GEOPHYSICS, **71**, No. 4, SI79–SI84.

Vasconcelos, I., and Snieder, R., 2008, Interferometry by deconvolution: Part 1 — theory for acoustic waves and numerical examples: GEOPHYSICS, **73**, No. 3, S115–S128.

Wapenaar, K., 2006, Seismic interferometry for passive and exploration data: Reconstruction of internal multiples, 2981–2985a.

Wapenaar, K., Draganov, D., Snieder, R., Campman, X., and Verdel, A., 2010, Tutorial on seismic interferometry. part i: Basic principles and applications: Geophysics, **75**, 75A195–75,209.

Weaver, R., and Lobkis, O., 2001, Ultrasonics without a source: Thermal fluctuation correlations at mhz frequencies: Physical Review Letters, **87**, No. 13.